Investigation of correlation between open-circuit voltage deficit and carrier recombination rates in Cu(In,Ga)(S,Se)$_2$-based thin-film solar cells

Jakapan Chantana,[1,a)] Takuya Kato,[2] Hiroki Sugimoto,[2] and Takashi Minemoto[1,a)]

[1]*Department of Electrical and Electronic Engineering, Ritsumeikan University, 1-1-1 Nojihigashi, Kusatsu, Shiga 525-8577, Japan*
[2]*Atsugi Research Center, Solar Frontier K. K., Atsugi, Kanagawa 243-0206, Japan*

The temperature-illumination-dependent open-circuit voltage (V_{OC}) method is utilized to separately and quantitatively estimate carrier recombination rates at the buffer/absorber interface, in the space-charge region (SCR), and in the quasi-neutral region (QNR) of Cu(In,Ga)(S,Se)$_2$ (CIGSSe)-based thin-film solar cells with various device structures. The correlation between open-circuit voltage deficits ($V_{OC,def}$) among the carrier recombination rates of the CIGSSe solar cells with a conversion efficiency (η) above 17% is examined. It is revealed that $V_{OC,def}$ is decreased to 0.373 V with the reduced carrier recombination rate at the buffer/absorber interface through the development of device structures. To further decrease $V_{OC,def}$ (for the improved η), the carrier recombination rates in SCR and QNR are essential to be reduced by the further improvement of CIGSSe quality. Consequently, understanding the quantitative carrier recombination rates across the device, estimated from the temperature-illumination-dependent V_{OC} method, is practical to know which part of the solar cell needs to be developed for high η above 20%. *Published by AIP Publishing.*
https://doi.org/10.1063/1.5023828

Thin-film solar cells are promising to reduce the production cost.[1,2] The conversion efficiency (η) above 20% for polycrystalline chalcopyrite Cu(In,Ga)Se$_2$ (CIGSe) and Cu(In,Ga)(S,Se)$_2$ (CIGSSe)-based thin-film solar cells with a lab-scale area has been reported by several research groups.[3–6] Moreover, CIGSe and CIGSSe-based photovoltaic (PV) modules have been already produced on a large scale and claimed to have long-term reliability.[7,8] It is well known that the η of the solar cells can be further enhanced when their open-circuit voltage deficit ($V_{OC,def}$), which is governed by recombination losses across the devices, is reduced.[9,10] Therefore, the method to minimize the carrier recombination losses has been intensively studied.[11–15] It has been reported that conduction band offsets of the buffer/absorber interface and the transparent conductive oxide/absorber interface in the solar cells play an important role in reducing the interface carrier recombination.[11–14] In addition, the reduction of defects in the absorber gives rise to a decrease in the carrier recombination rates in the space-charge region (SCR) and quasi-neutral region (QNR).[15] Therefore, the method, separately quantifying the carrier recombination rates at the buffer/absorber interface in SCR and in QNR in the solar cell, is important to understand the state-of-the-art and future improvements of cell performances.

Temperature-dependent open-circuit voltage (V_{OC}) is normally utilized to identify the dominant carrier recombination mechanism by the activation energy of recombination (E_A),[16,17] which is used to qualitatively assess the interface carrier recombination. It has been recently reported that the temperature-illumination-dependent V_{OC} method is capable of separately quantifying the recombination rates at the buffer/absorber interface, in SCR, and in QNR.[10,18]

In this work, the carrier recombination rates at the buffer/absorber interface, in SCR, and in QNR of the CIGSSe solar cells with various structures were quantitatively estimated based on the temperature-illumination-dependent V_{OC} method.[10,18] Moreover, the correlation between $V_{OC,def}$ and carrier recombination rates of the CIGSSe solar cells was examined.

Here, CIGSSe solar cells with different structures for various $V_{OC,def}$ values, where their η is above 17%, were characterized. Namely, CdS, Cd$_{0.75}$Zn$_{0.25}$S, ZnS(O,OH), and Zn$_{1-x}$Mg$_x$O layers as buffer layers were used, and ZnO:Al and Zn$_{1-x}$Mg$_x$O:Al as transparent conductive oxide (TCO) layers were utilized in the CIGSSe solar cells, where the Mg contents (x) of Zn$_{1-x}$Mg$_x$O buffer layers and Zn$_{1-x}$Mg$_x$O:Al (TCO) layers were varied from 0 to 0.4 and from 0 to 0.2, respectively.[14,19,20] The details of the cell fabrication process are described in our previous work.[14,19,20] It is noted that the near-surface bandgap energy (E_g) of all CIGSSe absorbers is about 1.30 eV. The cell performance parameters, which are short-circuit current density (J_{SC}), V_{OC}, fill factor (FF), and η, of the CIGSSe solar cells without anti-reflective coating layers (a designated area of 0.5 cm^2) were evaluated under Air Mass 1.5G illumination. The external quantum efficiency (EQE) of the solar cells was measured using the measurement system (CEP-25RR Bunkoukeiki). The minimum bandgap energy of all CIGSSe absorbers (E_{gmin}), which is 1.08 eV, was calculated from the first derivative of EQE (d(EQE)/dλ). λ denotes the wavelength.

Temperature dependent current density-voltage (J-V) characteristics were additionally performed under Air Mass 1.5G illumination using a cryostat cooled with liquid-N$_2$ and heated using a temperature controller (Scientific Instruments, Model 9700). The graph of V_{OC} as a function of temperature (T) (V_{OC}-T) presents a straight line, and the extrapolation of

a)jakapan@fc.ritsumei.ac.jp and minemoto@se.ritsumei.ac.jp

this line to T at 0 K leads to qV_{OC} at T = 0 K, defined as E_A.[16,17] The illumination dependence of V_{OC} (Suns-V_{OC}) was characterized by WCT–120 (Sinton Instruments). To measure the carrier density (N_A) of the CIGSSe absorber and built-in potential (φ_{bi}), the capacitance–voltage (C–V) measurement on CIGSSe solar cells was performed using a LCR meter (Hewlett Packard 4284A) with a frequency and an amplitude of 4 kHz and 10 mV, respectively.

Figure 1 illustrates the η of the resulting CIGSSe solar cells with different device structures as a function of $V_{OC,def}$. It is revealed that the decrease in $V_{OC,def}$ gives rise to the strong enhancement of η. Therefore, the correlation between $V_{OC,def}$ and carrier recombination rates of the CIGSSe solar cells is interestingly examined. Figure 2 shows $V_{OC,def}$ as functions of E_A and φ_{bi} of the CIGSSe solar cells. Since some E_A values are higher than E_{gmin} (approximately 1.08 eV) and the near-surface E_g of CIGSSe absorbers has strong influence on V_{OC},[21–23] the E_A of the CIGSSe solar cells is compared to the near-surface E_g (about 1.30 eV) in this work. In Fig. 2(a), $V_{OC,def}$ is decreased when the E_A is enhanced and closer to the near-surface E_g, thereby implying that the carrier recombination at the interface is reduced.[16,17] Moreover, $V_{OC,def}$ is reduced when φ_{bi} is increased in Fig. 2(b). It is considered that E_A is close to the near-surface E_g, implying low interface recombination or low interface defect states. With the increasing interface defect states, E_A is therefore lower than the near-surface E_g, and the charge at the interface, accumulated at the defects, is formed, thus decreasing φ_{bi}. According to Fig. 2, both E_A and φ_{bi} can be therefore used as indictors of the interface carrier recombination. However, the techniques using E_A and φ_{bi} are only utilized to qualitatively assess the interface recombination. To evaluate the state-of-the-art solar cells, the carrier recombination rates at the buffer/absorber interface, in SCR, and in QNR are vital to be separately quantified.

The carrier recombination rates at the buffer/absorber interface (R^i), in SCR (R^d), and in QNR (R^b) are therefore investigated based on the temperature-illumination-dependent V_{OC} method.[10,18] The 20.1%-efficient CIGSSe solar cell with a structure of Glass/Mo/CIGSSe/Cd$_{0.75}$Zn$_{0.25}$S/Zn$_{0.8}$Mg$_{0.2}$O/Zn$_{0.9}$Mg$_{0.1}$O:Al/Ni-Al is used as an example to estimate R^i, R^d, and R^b. Therefore, Fig. 3 demonstrates (a)

FIG. 2. $V_{OC,def}$ as functions of (a) E_A and (b) φ_{bi} for the CIGSSe solar cells with different structures. $V_{OC,def}$ is defined as E_{gmin}/q-V_{OC}. E_{gmin} and near-surface E_g of all CIGSSe absorbers are about 1.08 and 1.30 eV, respectively.

the photo-J-V characteristic and (b) EQE and d(EQE)/dλ of the 20.1%-efficient CIGSSe solar cell. In Fig. 3(b), the E_{gmin} of the CIGSSe absorber is approximately 1.08 eV, which was obtained from d(EQE)/dλ. According to Li *et al.*, R^i, R^d, and R^b can be expressed as[10,18]

$$R^i = R^i_0 \exp\left(\frac{qV}{kT}\right), \quad R^d = R^d_0 \exp\left(\frac{qV}{2kT}\right), \quad \text{and}$$

$$R^b = R^b_0 \exp\left(\frac{qV}{kT}\right), \tag{1}$$

where R^i_0, R^d_0, and R^b_0 are voltage-independent recombination rates at the buffer/absorber interface, in SCR, and in QNR, respectively. Moreover, V_{OC} and E_A are written as[10,18]

$$V_{OC} = \frac{2kT}{q} \ln\left[\frac{1}{2}\frac{R^d_0}{R^i_0 + R^b_0}\left(\sqrt{4GW\frac{R^i_0 + R^b_0}{(R^d_0)^2} + 1} - 1\right)\right] \tag{2}$$

and

$$E_A = \frac{R^i_0 q\varphi_{bo} + R^b_0 E_g}{R^i_0 + R^b_0}, \tag{3}$$

where φ_{bo} represents the potential barrier at the buffer/absorber interface at zero bias. φ_{bo} is obtained by $\varphi_{bi} + (E_F - E_V)$, where E_F and E_V are the Fermi energy and valence band maximum, respectively.[10,18] G is the illumination intensity (or optical generation), and W is the CIGSSe
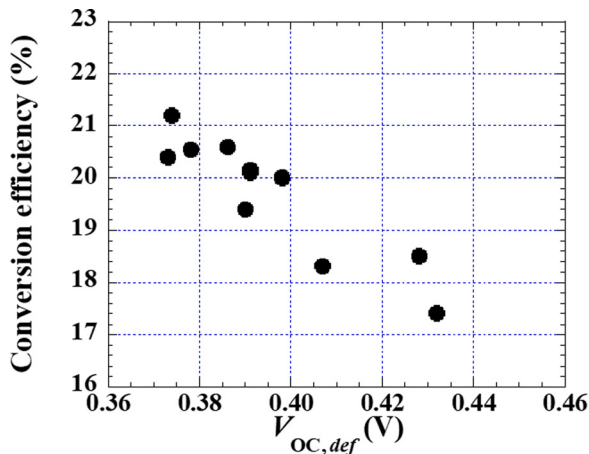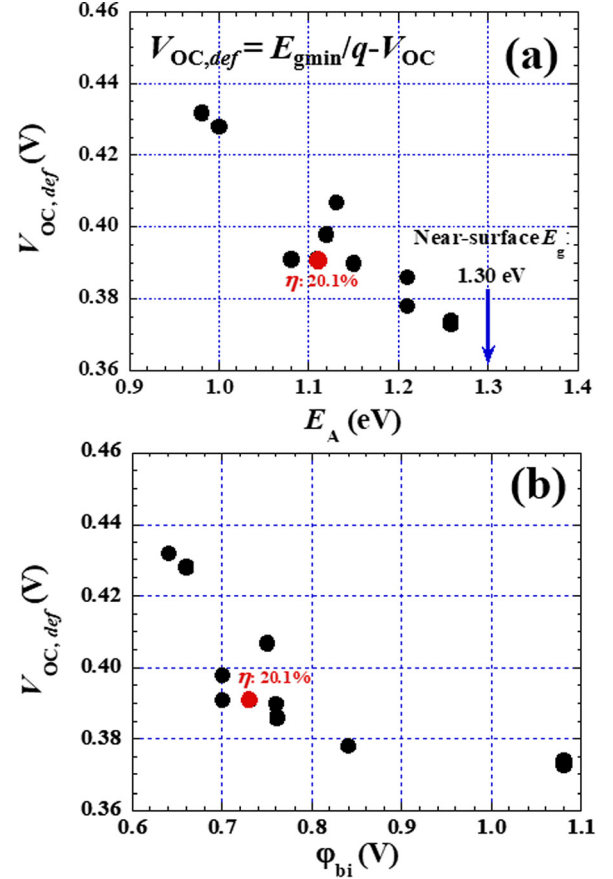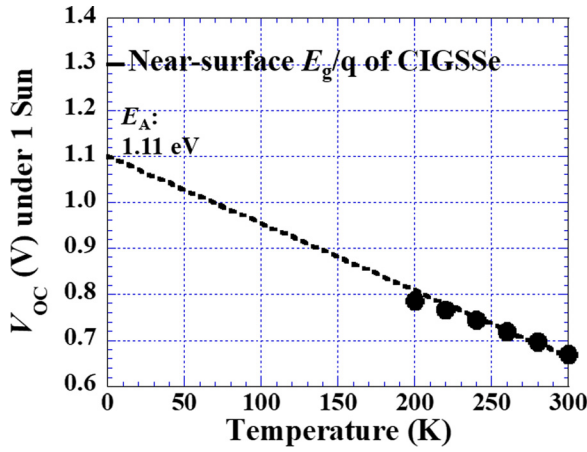

FIG. 1. Conversion efficiency of the CIGSSe solar cells with different device structures as a function of $V_{OC,def}$.

FIG. 3. (a) Photo-*J-V* characteristic and (b) EQE and d(EQE)/dλ of the 20.1%-efficient CIGSSe solar cell with a structure of Glass/Mo/CIGSSe/Cd$_{0.75}$Zn$_{0.25}$S/Zn$_{0.8}$Mg$_{0.2}$O/Zn$_{0.9}$Mg$_{0.1}$O:Al/Ni-Al. λ denotes the wavelength.

FIG. 4. Band diagram of the CIGSSe solar cell at zero bias ($V = 0$ V) demonstrating all relevant parameters.

FIG. 5. Dependence of V_{OC} on light-intensity G (Suns-V_{OC}) for the 20.1%-efficient CIGSSe solar cell with a structure of Glass/Mo/CIGSSe/Cd$_{0.75}$Zn$_{0.25}$S/Zn$_{0.8}$Mg$_{0.2}$O/Zn$_{0.9}$Mg$_{0.1}$O:Al/Ni-Al. R denotes the correlation coefficient, indicating how well the calculated curve fits the original data.

thickness (2 μm). Figure 4 consequently depicts all relevant parameters in a band diagram at zero bias. Based on Eq. (3), R^i_0/R^b_0 can be estimated, where E_g used in Eq. (3) is near-surface E_g of the CIGSSe absorber, which is 1.30 eV in this work.

To extract R^i_0, R^d_0, and R^b_0, V_{OC} as a function of light-intensity G (Suns-V_{OC}) is first investigated in Fig. 5. The measured V_{OC} as a function of G in Fig. 5 is then fitted using Eq. (2) to estimate R^d_0 and $R^i_0 + R^b_0$ in Table I. From Fig. 6, the E_A of 1.11 eV is obtained in Table I. Based on the $C-V$ measurement for the Mott-Schottky plot, N$_A$, φ_{bi}, $(E_F - E_V)/q$, and φ_{bo} are extracted in Table I. $(E_F - E_V)/q$ was estimated from the effective density of states of the valence band (N$_V$) of 1.8×10^{19} cm^{-3} taken from (Ref. 10), where $(E_F - E_V)/q$ is equal to kT/q ln (N$_V$/N$_A$). R^i_0/R^b_0 is consequently obtained using Eq. (3). In Table I, the φ_{bi} and E_A values of the 20.1%-efficient CIGSSe solar cell are demonstrated in Fig. 2 as red data points. It is shown that the relatively high E_A of 1.11 eV and φ_{bi} of 0.73 V lead to the decrease in $V_{OC,def}$ to 0.391 V in Table II. To develop CIGSSe solar cells, carrier recombination rates are essential to be quantified. The R^i_0, R^d_0, and R^b_0 of the 20.1%-efficient CIGSSe solar cell were consequently calculated and are given in Table II. The corresponding R^i, R^d, and R^b in Table II were calculated using Eq. (1) at $V = V_{OC}$. As a result, R^i, R^d, and R^b can be practically obtained based on the temperature-illumination-dependent V_{OC} method.[10,18]

Next, the correlation between $V_{OC,def}$ and the resulting carrier recombination rates of the various CIGSSe solar cells with different structures was examined. R^i_0, R^d_0, R^b_0, R^i, R^d, and R^b were estimated based on the temperature-illumination-dependent V_{OC} method.[10,18] Figure 7 therefore demonstrates

TABLE I. Essential parameters for extracting R^i_0, R^d_0, and R^b_0 for the 20.1%-efficient CIGSSe solar cell with a structure of Glass/Mo/CIGSSe/Cd$_{0.75}$Zn$_{0.25}$S/Zn$_{0.8}$Mg$_{0.2}$O/Zn$_{0.9}$Mg$_{0.1}$O:Al/Ni-Al, which were obtained from V_{OC}-T, Suns-V_{OC}, and $C-V$ measurements. Near-surface E_g is the near-surface bandgap energy (1.3 eV) of the CIGSSe absorber.

R^d_0 (cm^{-2} s^{-1})	$R^i_0 + R^b_0$ (cm^{-2} s^{-1})	Near-surface E_g (eV)	E_A (eV)	N$_A$ (cm^{-3})	φ_{bi} (V)	$(E_F - E_V)/q$ (V)	φ_{bo} (V)	R^i_0/R^b_0
4.91×10^{11}	6.72×10^5	1.30	1.11	1.10×10^{16}	0.73	0.192	0.922	0.986

FIG. 6. V_{OC} as a function of temperature for the 20.1%-efficient CIGSSe solar cell with a structure of Glass/Mo/CIGSSe/$Cd_{0.75}Zn_{0.25}S$/$Zn_{0.8}Mg_{0.2}O$/$Zn_{0.9}Mg_{0.1}O$:Al/Ni-Al. The near-surface E_g of the CIGSSe absorber is about 1.30 eV.

FIG. 7. R^i_0, R^d_0, and R^b_0 as a function of $V_{OC,def}$ for several CIGSSe solar cells with different device structures.

R^i_0, R^d_0, and R^b_0 as a function of $V_{OC,def}$ for the several CIGSSe solar cells with different structures ($\eta > 17\%$). It is revealed that R^d_0 and R^b_0 are almost constant, while R^i_0 is most changed with the variation of $V_{OC,def}$ through the development of the device structure. $V_{OC,def}$ is significantly minimized with the decrease in R^i_0. The lowest $V_{OC,def}$ of 0.373 V is achieved with the lowest R^i_0 (7.04×10^3 cm^{-2} s^{-1}). It is disclosed that R^i_0 is most influenced and minimized by developing a device structure. To further minimize $V_{OC,def}$ lower than 0.373 V, it is suggested that the research should focus on the improvement of CIGSSe quality (low defect) in order to minimize the carrier recombination rates in SCR and QNR (R^d_0 and R^b_0).

Moreover, Fig. 8 demonstrates (a) R^i, R^d, and R^b and (b) their values normalized with R^b (normalized carrier recombination rates) since CIGSSe quality is almost similar (or almost similar R^b). The relatively high $V_{OC,def}$ (above 0.428 V) is demonstrated in the solar cells with the normalized carrier recombination rates at the buffer/absorber interface and in SCR higher than that in QNR. On the other hand, the relatively low $V_{OC,def}$ (below 0.391 V) is normally shown in the solar cells with the normalized carrier recombination rates at the buffer/absorber interface and in SCR lower than that in QNR. Moreover, $V_{OC,def}$ is further decreased to the lowest (0.373 V) when the normalized carrier recombination rate at the buffer/absorber interface is far lower than those in SCR and QNR, mainly achieved by the development of device structures. According to the results, the temperature-illumination-dependent V_{OC} method, which can separately quantify the carrier recombination rates at the buffer/absorber interface in SCR and in QNR, is practical to understand that which part of the solar cell needs to be further improved for high η above 20%.
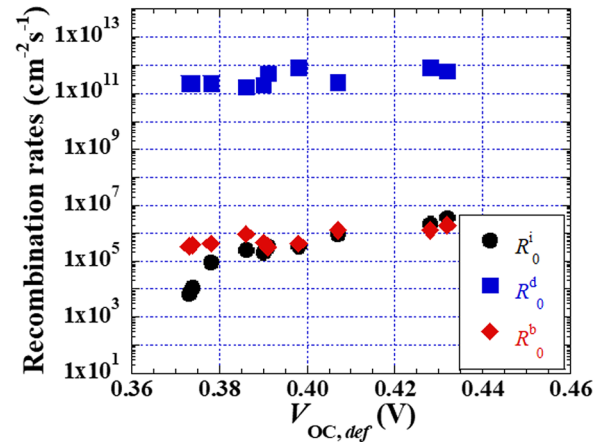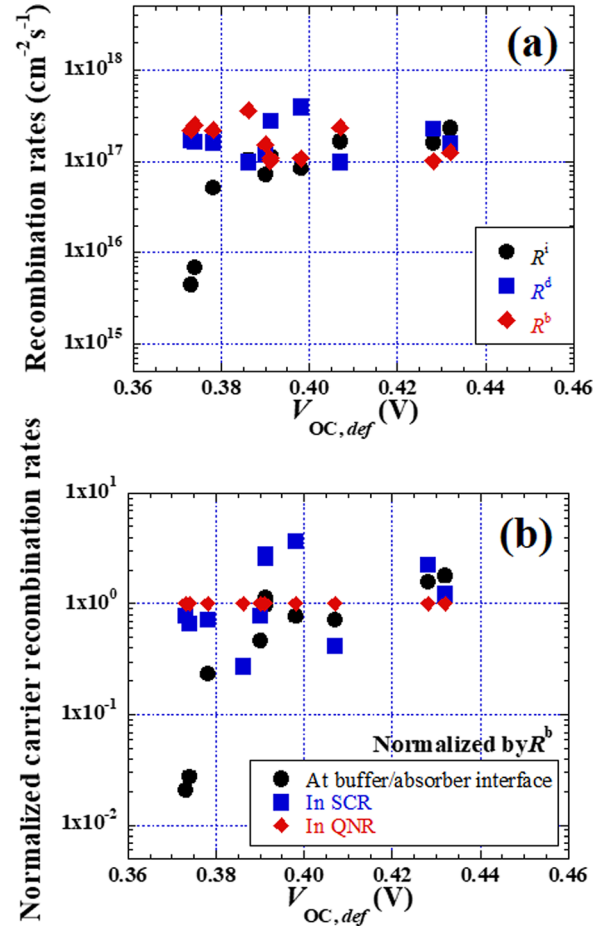

FIG. 8. (a) R^i, R^d, and R^b and (b) their values normalized with R^b (normalized carrier recombination rates) as a function of $V_{OC,def}$ for the various CIGSSe solar cells with different device structures.

TABLE II. Summary of device performances of the 20.1%-efficient CIGSSe solar cell with a structure of Glass/Mo/CIGSSe/$Cd_{0.75}Zn_{0.25}S$/$Zn_{0.8}Mg_{0.2}O$/$Zn_{0.9}Mg_{0.1}O$:Al/Ni-Al and the extracted recombination parameters. The open-circuit-voltage deficit ($V_{OC,def}$) is defined as E_{gmin}/q-V_{OC}. E_{gmin} (1.08 eV) is the bandgap energy of the CIGSSe absorber obtained from the first derivative of EQE of the solar cell.

η (%)	V_{OC} (V)	$V_{OC,def}$ (V)	R^i_0 (cm^{-2} s^{-1})	R^d_0 (cm^{-2} s^{-1})	R^b_0 (cm^{-2} s^{-1})	R^i (cm^{-2} s^{-1})	R^d (cm^{-2} s^{-1})	R^b (cm^{-2} s^{-1})
20.1	0.689	0.391	3.34×10^5	4.91×10^{11}	3.38×10^5	1.08×10^{17}	2.79×10^{17}	1.09×10^{17}

In summary, the temperature-illumination-dependent V_{OC} method can practically and separately quantify the recombination rates at the buffer/absorber interface, in SCR, and in QNR. The relationships of $V_{OC,def}$ among the carrier recombination rates for the CIGSSe solar cells with different structures are demonstrated. It is disclosed that the carrier recombination rate at the buffer/absorber interface is most influenced by developing a device structure, whereas the carrier recombination rates in SCR and QNR are almost constant. As a result, the lowest $V_{OC,def}$ of 0.373 V is achieved with the lowest R^i_0 (7.04×10^3 cm^{-2} s^{-1}).

[1]Y. Hamakawa, *Thin-Film Solar Cells Next Generation Photovoltaics and Its Applications*, edited by Y. Hamakawa (Springer, Heidelberg, 2004), p. 1.

[2]E. Vallat-Sauvain, A. Shah, and J. Bailat, *Thin Film Solar Cells, Fabrication, Characterization and Applications*, edited by J. Poortmans and V. Arkhipov (Wiley, Chichester, 2006), p. 133.

[3]A. Chirila, P. Reinhard, F. Pianezzi, P. Bloesh, A. R. Uhl, C. Fella, L. Kranz, D. Keller, C. Gretener, H. Hagendorfer, D. Jaeger, R. Erni, S. Nishiwaki, S. Buecheler, and A. N. Tiwari, Nat. Mater. **12**, 1107 (2013).

[4]P. Jackson, D. Hariskos, R. Wuerz, O. Kiowski, A. Bauer, T. M. Friedmeiwe, and M. Powalla, Phys. Status Solidi RRL **9**, 28 (2015).

[5]P. Jackson, R. Wuerz, D. Hariskos, E. Lotter, W. Witte, and M. Powalla, Phys. Status Solidi RRL **10**, 583 (2016).

[6]See http://www.solar-frontier.com/eng/news/2017/1220_press.html for World Record Thin-Film Solar Cell Efficiency: 22.9%, Solar Frontier.

[7]S. Niki, M. Contreras, I. Repins, M. Powalla, K. Kushiya, S. Ishizuka, and K. Matsubara, Prog. Photovoltaics Res. Appl. **18**, 453 (2010).

[8]H. Sugimoto, in *Proceeding of the 40th IEEE Photovoltaic Specialists Conference*, Denver, 2014, p. 2767.

[9]M. A. Contreras, L. M. Mansfied, B. Egass, J. Li, M. Romero, R., Noufi, E. Rudiger-Voigt, and W. Mannstadt, Prog. Photovoltaics: Res. Appl. **20**, 843 (2012).

[10]J. V. Li, S. Grover, M. A. Contreras, K. Ramanathan, D. Kuciauskas, and R. Noufi, Sol. Energy Mater. Sol. Cells **124**, 143 (2014).

[11]T. Minemoto, T. Matsui, H. Takakura, Y. Hamakawa, T. Negami, Y. Hashimoto, T. Uenoyama, and M. Kitagawa, Sol. Energy Mater. Sol. Cells **67**, 83 (2001).

[12]T. Nakada, M. Hongo, and E. Hayashi, Thin Solid Films **431–432**, 242 (2003).

[13]M. Murata, J. Chantana, N. Ashida, D. Hironiwa, and T. Minemoto, Jpn. J. Appl. Phys., Part 1 **54**, 032301 (2015).

[14]J. Chantana, T. Kato, H. Sugimoto, and T. Minemoto, Prog. Photovoltaics Res. Appl. **25**, 996 (2017).

[15]J. T. Heath, J. D. Cohen, W. N. Shafarman, D. X. Liao, and A. A. Rockett, Appl. Phys. Lett. **80**, 4540 (2002).

[16]M. Turcu, O. Pakma, and U. Rau, Appl. Phys. Lett. **80**, 2598 (2002).

[17]K. Tanaka, T. Minemoto, and H. Takakura, Sol. Energy **83**, 477 (2009).

[18]S. Grover, J. V. Li, D. L. Young, P. Stradins, and H. W. Branz, Appl. Phys. Lett. **103**, 093502 (2013).

[19]J. Chantana, T. Kato, H. Sugimoto, and T. Minemoto, Prog. Photovolaics Res. Appl. **25**, 431 (2017).

[20]J. Chantana, T. Kato, H. Sugimoto, and T. Minemoto, Prog. Photovolaics Res. Appl. **26**(2), 127–134 (2018).

[21]J. Chantana, T. Watanabe, S. Teraji, K. Kawamura, and T. Minemoto, Appl. Phys. Lett. **103**, 223901 (2013).

[22]J. Chantana, D. Hironiwa, T. Watanabe, S. Teraji, K. Kawamura, and T. Minemoto, Thin Solid Films **582**, 7 (2015).

[23]J. Chantana, D. Hironiwa, T. Watanabe, S. Teraji, K. Kawamura, and T. Minemoto, Renewable Energy **76**, 575 (2015).